Preparation and characterization of polysulfone–cyclodextrin composite nanofiltration membrane: Solvent effect

ARTICLE *in* JOURNAL OF APPLIED POLYMER SCIENCE · SEPTEMBER 2012

Impact Factor: 1.77 · DOI: 10.1002/app.36711

4 AUTHORS, INCLUDING:

Kundan Baruah
Gauhati University
7 PUBLICATIONS **11** CITATIONS

SEE PROFILE

Swapnali Hazarika
Council of Scientific and Industrial Research …
21 PUBLICATIONS **173** CITATIONS

SEE PROFILE

Preparation and Characterization of Polysulfone–Cyclodextrin Composite Nanofiltration Membrane: Solvent Effect

Kundan Baruah, Swapnali Hazarika,* Somiron Borthakur, Narendra Nath Dutta

Chemical Engineering Division, CSIR—North East Institute of Science and Technology, Jorhat 785006, Assam, India

Received 11 August 2011; accepted 31 December 2011
DOI 10.1002/app.36711
Published online in Wiley Online Library (wileyonlinelibrary.com).

ABSTRACT: α-Cyclodextrin membranes were prepared by the phase inversion method using four types of casting solvents such as N-methyl pyrrolidone (NMP), dimethyl sulfoxide (DMSO), dimethyl acetamide (DMAc), and dimethyl formamide (DMF) herein-after termed as α-CD-NMP, α-CD-DMSO, α-CD-DMAc, and α-CD-DMF, respectively. The membranes were characterized by IR, XRD, TGA-DTA, DSC, and SEM analysis and show that solvents like NMP, DMA, DMF give good uniform morphological membranes and are better than that of DMSO. Thermal decompositions of the pure polymer and composite membranes indicate different range of thermal degradation of the membrane. This study reveals that the casting solvents NMP, DMF, DMAC have nearly same significant effect on morphology and other properties of the membranes. This is explained in terms of demixing behavior of the polymer and the combined effect of solvent volatility and polymer–solvent interactions as estimated from Hansen solubility parameter. Solvent hydrophobicity also affects the performance of the membrane and can be determined in terms of water permeability. © 2012 Wiley Periodicals, Inc. J Appl Polym Sci 000: 000–000, 2012

Key words: α-cyclodextrin; NF membrane; solvent effect; membrane morphology; Hansen solubility parameter

INTRODUCTION

Nanofiltration is a relatively new membrane separation technique which is a pressure-driven membrane process normally applicable for separation of dissolved components. The speciality of NF membrane is water softening, treatment of industrial effluents contaminated with organics or heavy metals.[1–4] The process is regarded as an innovative and promising water treatment technique, and a potential alternative to conventional water treatment approaches.[5–7] Most NF membranes are composite in nature, with a selective layer on the top of the microporous substrate. Many researchers have developed several methods for preparation of selective layer through polymerization.[8,9]

To make a high-performance separation membrane, it is essential to study the membrane formation procedure which is an important issue in membrane research. The thermodynamic properties of the casting solution and coagulation pairs play a very important role on the structure and performance of a membrane prepared by immersion precipitation.[10,11] Different ternary systems result in different membranes with different structures.[12,13] Tight NF membrane has a smaller pore size, which is usually adopted for water softening. Properties of solvent can also affect the membrane morphology and performance of membrane. Addition of a volatile solvent along with a non-solvent can change liquid–liquid behavior and as a result membrane morphology may be changed. Again addition of a co-solvent to a polymeric solution can eliminate macrovoid formation during instantaneous demixing and change the morphology of the membrane from finger-like to sponge-like structure. Boussu et al.[14] studied the polyethersulfone membrane using DMF and NMP on the casting solvent. This self-made membrane has very good retention for charged compounds in combination with high-permeate flux.

In our present work, we have considered α-cyclodextrin (α-CD) as novel polymer for preparation of NF membrane which is composite with polysulfone. Cyclodextrins are macrocyclic oligomers of α-D-glucose and they are shaped like truncated cones with primary and secondary hydroxyl groups crowning the narrower rim and wider rim respectively. In CD, the glucose units are arranged in such a way that the hydroxymethylene groups are pointing downward, whereas the hydroxyl groups are pointing upward. As a result of this, a hydrophilic outer space and a hydrophobic inner space are formed leading to the particular ability of the cyclodextrins to form host–guest complexes with organic components having appropriate diameters and physical interactions.[15,16] It is also used as supramolecular carrier in organometallic reactions and other

*Correspondence to: S. Hazarika (shrrljt@yahoo.com).

TABLE I
Composition and Physical Properties of α-CD Membrane in Different Solvent

Solvent	Membrane thickness (μm)	Pore diameter (nm)	Surface porosity (ε%)	Pure water permeability ($Lm^{-2}h^{-1}$)	Water uptake (%)	Contact angle (°)
NMP	57.40	1.26	0.19	48	8.36	38
DMAc	13.40	1.64	0.30	40	6.05	41
DMF	76.80	1.81	0.59	32	5.43	49
DMSO	86.70	2.11	0.22	20	3.21	57

Weight of α-CD = 0.3678%; weight of polysulfone = 10.9874%; weight of additive = 1.0999%; Weight of $LiNO_3$ = 0.1857%; Weight of solvent added = 87.3592%

areas.[17,18] To get better understanding of the binding events, a lot of theoretical and experimental methods have been used to study the CD complexes. CD is expected to provide good membrane morphology; however, a very limited study is available in literature. Hence we attempted to study the membrane formation capability of CD composite with polysulfone. In our work, we have been studying the solvent effect on preparation of NF membrane from CD composite with polysulfone and their characterization through investigating the effect of pore size of the membranes in different solvents by measuring pure water permeate flux.

MATERIALS AND METHODS

Chemicals

Commercial grade polysulfone (average mol. wt. 27,000) was supplied by Aldrich Chemical Company, USA. Polyethylene glycol (PEG 1500) was obtained from G. S. Chemical testing and allied industries. Inorganic salt lithium nitrate and α-cyclodextrin were supplied from Acros Organics, USA. *N*-methyl pyrrolidone (NMP) was supplied by RANBAXY Fine Chemicals, New Delhi. *N*,*N*-dimethyl formamide (DMF) and *N*,*N*-dimethyl acetamide (DMAc) were supplied by Acros Organics. Dimethyl sulfoxide (DMSO) was purchased from MERCK India, Bombay. Deionized water was used as coagulation bath.

Methods

Preparation of membrane

Flat sheet membranes are prepared by phase inversion method. Polysulfone (PSf) is mixed with a definite amount of α-cyclodextrin, polyethylene glycol, $LiNO_3$, and then dissolved in different solvents viz., NMP, DMF, DMAc, and DMSO separately at room temperature (28–32°C and relative humidity about 78%) to make the casting solution. The polymer solution is stirred for about 6 h at room temperature (28–27°C) using a magnetic stirrer until a homogeneous solution was achieved. Film was cast on a glass plate with a casting knife of thickness 0.5 mm maintaining the same temperature as in the solution and are exposed for about 5 min to ambient before immersion into a coagulation bath that contains ice-cooled water (maintained at about 6°C). When the cast films changed their color from transparent to white, immediately the plate is immersed into the coagulation bath and the films were separated out from the glass plate after some time. The prepared membrane sheets were washed under running water and kept in deionized water bath overnight. Then the sheets were dried at room temperature. Finally the membranes were characterized by using different analytical methods and kept ready for permeation experiments.

The casted membranes were then characterized for porosimetry measurement by standard pressure. The surface morphology and thickness of the membranes were determined by SEM. Pure water permeability for all membranes were measured in a membrane cell of standard design. The membrane with effective area 28.3 cm^2 was set in the cell and the pure water permeability test was carried out by applying a pressure of 4.9 bar pressure to the feed side. The quantity of water permeated through the membrane was measured as permeation rate.

Composition and physical properties such as membrane thickness, pore diameter, surface porosity, and pure water permeability of membranes are shown in Table I.

Characterization of membrane

Membranes were characterized by IR (PERKIN Elmer System 2000), NMR (ADVANCE DPX BRUKER 270 MHz), XRD (JDX-11P-3A, JEOL, Japan), TGA-DTA (Perkin Elmer PC series DSC 7), water uptake, contact angle, surface morphology, thickness, and pore diameter measurement.

Water uptake of the prepared membranes was determined by measuring the weight variation before and after the hydration. The membranes were immersed in deionized water at 27°C for 24 h. The surface water attached onto the membrane was removed and blotted with tissue paper before

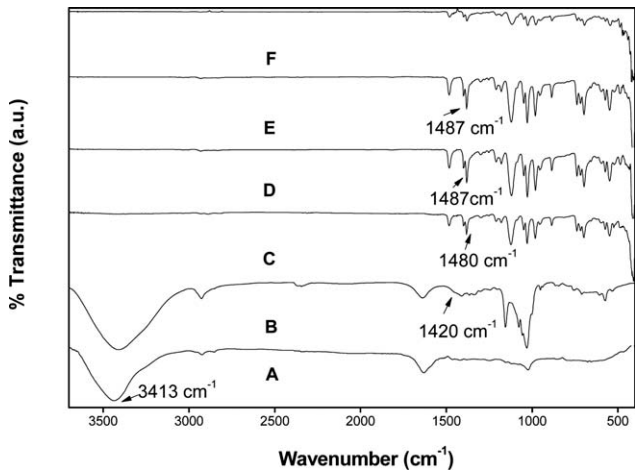

Figure 1 FTIR spectra of composite membranes and its components. A = α-cyclodextrin; B = polysulfone; C = *N*-methyl pyrrolidone; D = dimethyl formamide; E = dimethyl acetamide; F = dimethyl sulfoxide.

weighing the wet membranes to obtain W_{wet}. Then the wet membranes were dried under vacuum at 100°C overnight, weighed to obtain W_{dry}. The water uptake was calculated using the following equation:

$$\text{Water uptake} = (W_{wet} - W_{dry}/W_{dry}) \times 100\% \quad (1)$$

Contact angles of the membranes were measured by bubble formation method applying Poiseuille's equation which expresses the balance between viscous forces and capillary and hydrostatic forces (neglecting inertial effects).[19]

Membrane morphology was studied by a scanning electron microscope (LEO 1427VP, UK) which directly provides the visual information of the membrane morphology such as pore shape, size, their distribution, and density.

The thickness of the prepared membranes was measured by a membrane thickness gauge made by Mitutoyo Corporation, Japan.

Pore diameter of the membranes was determined by capillary condensation flow porometer (PMI, Model CCFP-5A). The principle of this process is that at a pressure P_o of vapor, in equilibrium with its liquid, can condense in pores of material. Vapor condenses in all pores smaller than D (pore diameter), determined by the pressure of the vapor[20]:

$$D = -[4\gamma_o r \cos\theta/RT)]/\ln(P/P_o) \quad (2)$$

where γ is the surface tension of condensed liquid, v is the molar volume of condensed liquid, Q is the contact angle of the liquid with the pore, D is the pore diameter, R is the gas constant, and T is the absolute test temperature. At the lowest relative vapor pressure, (P/P_o), condensation occurs in the smallest pore. On increase of relative vapor pressure condensation occurs in larger pores. A small increase in pressure on inlet side of the sample causes flow. Measurement of pressure change in outlet side of the sample yields flow rate:

$$F_{STP} = (\gamma_o T_s/Tp_s)(dp/dt) \quad (3)$$

After obtaining the value of vapor equilibrated with the sample and rates of pressure change, the pore diameters of the nanopore membrane were obtained.

RESULTS AND DISCUSSION

Primary effect

The interaction between residual solvents and α-cyclodextrin membrane

The FTIR spectra obtained for polysulfone, α-cyclodextrin, and the composite membranes in different casting solvents are shown in Figure 1. A broad peak is observed at 3413 cm^{-1} for α-CD indicates the presence of –OH group; however, this peak is found to be absent in the composite membrane of α-CD because of the interaction between the outer surfaces of α-CD molecule with the polar solvent. For composite membrane, the band in the range 3413–3434 cm^{-1} indicates the absence of aromaticity of α-CD, C=O stretching band is obtained in the range 1420–1580 cm^{-1} for α-CD-NMP, α-CD-DMAc, and α-CD-DMF membranes which is absent in α-CD-DMSO membrane. Other main bands appearing in the IR spectrum for polymer and composite membranes were assigned and tabulated separately in Table II.

A difference is also observed in ^{1}H-NMR of α-CD-NMP membrane where a very intense singlet appeared at 1.7 δ indicating a stronger interaction between α-CD and NMP compared with the others. The ^{1}H-NMR spectrums of the composite membranes are shown in Figure 2. All the four membranes show similar intense peaks at 1.61 ppm while some other peaks are also observed due to different chemical environment. The presence of residual solvent in the membrane casting is also identified from the ^{1}H-NMR spectra even though it is quite a trace amount, the signal at 2.1–2.9 ppm in the α-CD-NMP, α-CD-DMF, and α-CD-DMAc is attributed due to the free $–N(CH_3)_2$ group. From this observation, it can be concluded that the solvent plasticization effect on membrane properties is negligible as the residual solvent content is too small.[21] Also NMP is comparatively less volatile and hence resides on the membrane, indicated by the sharp intense peak at 3.51 ppm which is predicted to be due to the interaction of the solvent (NMP) with α-CD. The observation of intense peak in α-CD-NMP membrane can be attributed due to the strong H-bonding which is a main

TABLE II
Assignments of Main Adsorption Bands for Composite Membranes and Polymers

Sample	Vibrational frequency (cm^{-1})	Bond assignment
Polysulfone	3434	O—H str that may be arise due to absorption of water during analysis
	2327.79	CH_3 sym str
	1644.05	O—C aromatic ring str
	1018.81–1148	C—SO_2—C sym str
α-Cyclodextrin	3413.34	O—H str
	2327.79	C—C bend
	1411.25–1644.75	C—O str
	1153.17	C—O str (ethereal group)
α-CD-NMP	2850–3100	N—Hstr
	1584	C=O str
	1487.9	C—H str
	1105.2	C—C str
	1150	C—$S0_2$—C sym str
α-CD-DMF	3100–3500	N—H str
	1504–1580	C=O str
	1409–1487	C—H str
	1148–1168.6	C—SO_2—C sym str
	1013–1104	C—C aromatic str
α-CD-DMAc	3100–3500	N—H str
	1584.3–1504.9	C=O str
	1487–1404	C—H str
	1149–1104	C—SO_2—C sym str
	1013–1080.3	C—C bend
α-CD-DMSO	1582–1506	C=O bend
	1484	C—H str
	1323	S=O bend
	1146–1168	C—SO_2—C sym str
	1102	C—C bend

cause for the difference in membrane properties in different casting solvent. This peak is also present in α-CD-DMAc membrane.

The diffraction pattern of the membranes has been studied by XRD spectra and is shown in Figure 3. The X-ray investigation provided the information about the structural changes induced in α-CD-polysulfone composite membranes in four different solvents. The patterns for the four membranes showed broad peaks in the range of 7.40–10.12. From the figure, it is seen that the peak position does not depend on the casting solution. However, compared to other three membranes, the pattern of α-CD-NMP membrane shows a broadband peak with a decrease in peak intensity. Broad peak of the composite membrane indicates the amorphous state. The broad peaks also indicate the conformation of complete homogeneity and compatibility among the components of the membrane. This type of observation was reported by Guan et al.[21] for sulfonated polyethersulfone (SPES) membrane. The relative degree of the phase can be estimated from the full width at half maximum value (FWHM) given in Table III, wherein *d*-values and FWHM values are also shown. For α-CD-NMP membrane, FWHM value is 3.8, which is bigger than that of other values of FWHM of other membranes studied in this work. This indicates that stronger hydrogen bonding interaction occurred between α-CD-NMP membranes compared with that between other three solvents with α-CD. The values are different for SPES membrane in different casting solvents as reported by Guan et al.[21] For blend membranes with sulfonated polystyrene and sulfonated poly(2,6-dimethyl 1,4-phenylene oxide), the electrostatic cross-linking resulting from the ionic groups of sulfonated polymers increases the amorphous region abruptly.[22,23]

Effect of residual solvents on the thermal behavior of membrane

During the use of composite NF membranes, the stability of them against thermal stress is of great importance. Thus, thermogravimetric analysis was carried out under nitrogen atmosphere at a heating rate of 10°C min^{-1}. The decomposition curves of pure polymer and composite membranes are shown in Figure 4 wherein the derivative curves are shown in Figure 5. For polysulfone, two-step decompositions are at 473.39 and 608.50°C whereas four-step decompositions for α-CD are at 56.02, 127.54, 296.37, and 360.85°C, respectively. For α-CD-NMP, membrane four-step decompositions occur at 122.87, 177.16, 404.68, and 576.44°C whereas for other membranes decomposition occurs in two steps. The decomposition of α-CD-DMAc, α-CD-DMSO, and α-CD-DMF occurs at 465.80 and 576.85, 403.87 and 581.75, and 449.62 and 640.92°C, respectively. DSC measurements of the membranes were carried out at a heating rate of 10°C min^{-1} in nitrogen atmosphere. Melting endothermic peaks obtained at different temperatures for pure polymer and composite membrane were shown in Figure 6. The change in T_g for composite membranes was strongly influenced by the pore structure and can be explained by the percolation theory[24] which explains the glass transition behavior in polymer thin film. According to the percolation theory, the polymer sample is composed of domains of fast and slow dynamics, which are each approximately 2 nm in size. The population of slow domains is controlled by the sample temperature. The glass transition occurs on cooling due to the percolation of domains of slow dynamics by thermally induced density fluctuations. The domains of fast dynamics do not affect the overall viscosity. In nanoporous samples, a free-surface interfacial region that surrounds each nanopore results in high polymer chain mobility. These highly mobile regions are dispersed throughout the polymer matrix, and they contribute to the disruption of the percolation of the slow domains when the system is cooled from the polymer melt. In confined systems, such as

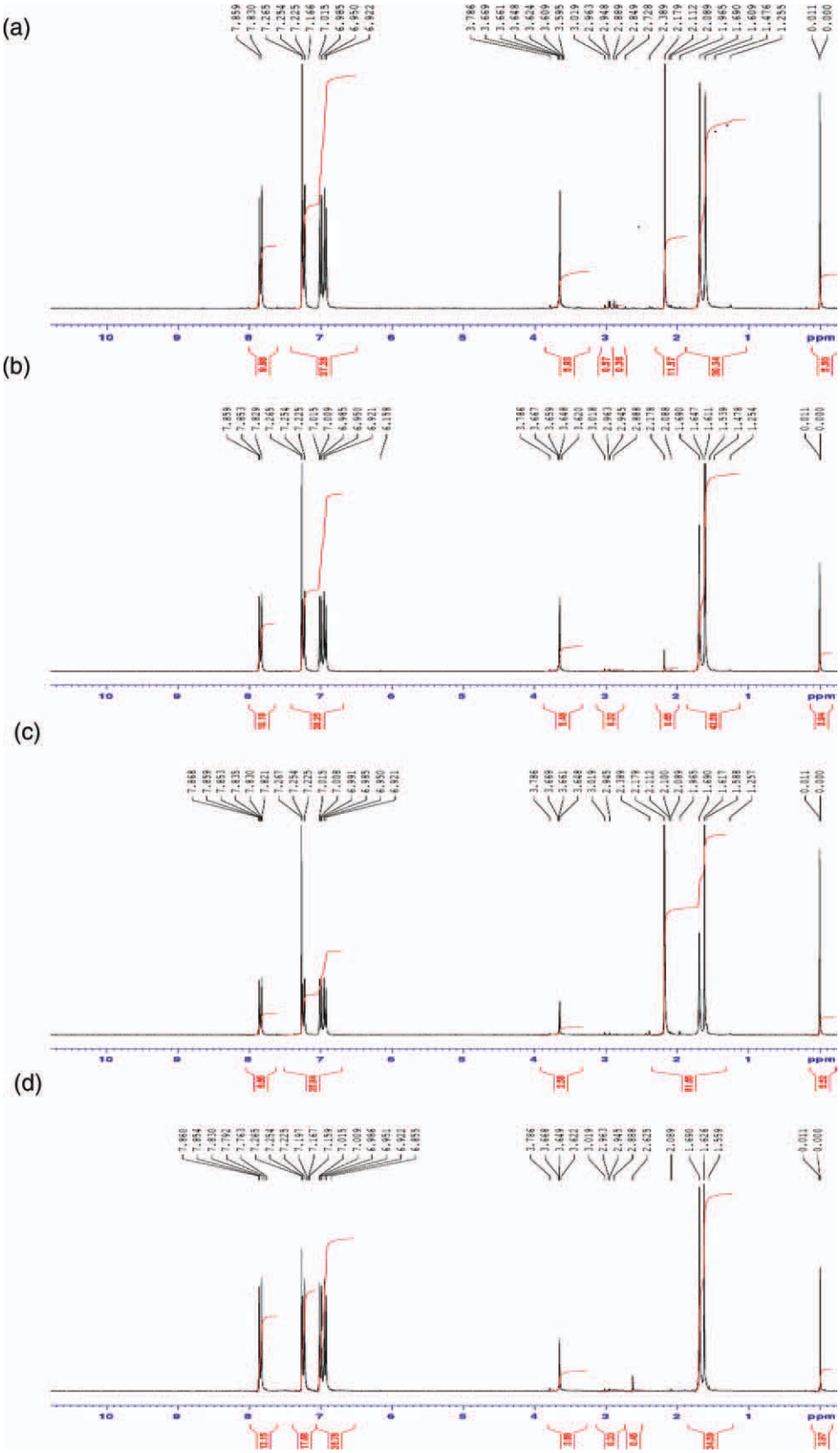

Figure 2 (a) ^{1}H-NMR spectra of α-CD-NMP membrane; (b): ^{1}H-NMR spectra of α-CD-DMF membrane; (c): ^{1}H-NMR spectra of α-CD-DMAc membrane; (d): ^{1}H-NMR spectra of α-CD-DMSO membrane. [Color figure can be viewed in the online issue, which is available at wileyonlinelibrary.com.]

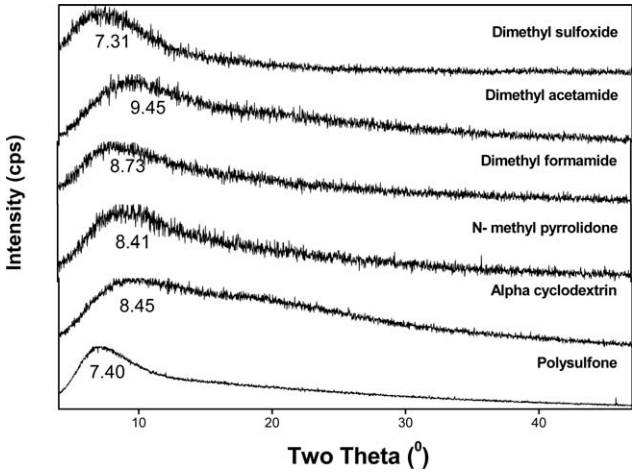

Figure 3 X-ray diffraction pattern of composite membranes.

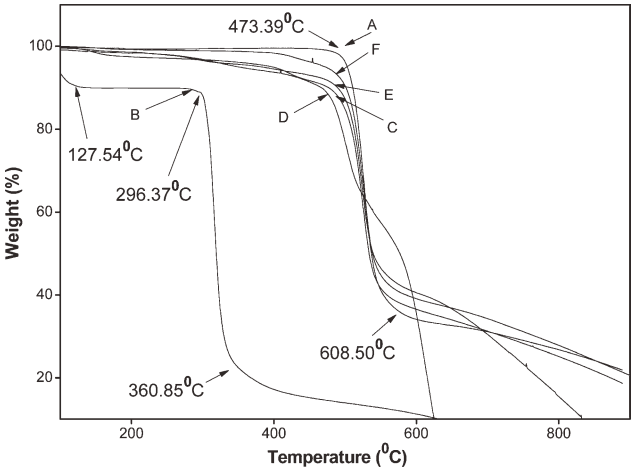

Figure 4 Thermogravimetric curves of polymer and composite membrane in different casting solvent, A = polysulfone, B = alpha cyclodextrin, C = CD-NMP, D = CD-DMF, E = CD-DMAc, F = CD-DMSO.

nanoporous polymers and polymer thin films, the interfacial regions are sufficiently close together that the percolation of the slow domains is restrained by these interfacial regions, and this causes the glass transition to occur at a lower temperature compared with that of the bulk polymer. For this reason, T_g value decreases in case of CD membranes than that of pure polymer. The T_g values for the composite membranes obtained from Figure 6 were plotted with respective pore diameter of the membranes which gives a linear relationship (Fig. 7) represented by following equation:

$$y = 58.021x - 42.243 \quad (4)$$

With a correlation co-efficient 0.97 which may be considered highly significant. The increase in T_g value indicates thermal stability of composite membrane probably due to the formation of van der Waals bonds that exist inside the cavity of α-CD and the H-bonding existing between residual –OH on α-CD in the respective solvent.

Effect of casting solvents on the surface morphologies of α-CD membranes

Membrane morphology for different α-CD membranes was studied by SEM analysis and is shown in Figure 8(a) and (b). Figure 8(a) shows the SEM image of the top surface of NF membranes in different casting solvents. The reason for such type of surface morphology may be explained from the concept of quaternary phase diagram of membrane formation.[24] A schematic phase diagram for ternary system is shown in Figure 9.[25] The morphology and properties of the membrane are strongly dependent on the dope position, critical point position, and precipitation path. When precipitation path crosses the binodal curve, phase separation starts with nucleation and growth of the polymer-rich or polymer-lean phase.[25] If the polymer concentration is low, the precipitation path crosses the equilibrium line below the critical point and nucleation of a polymer-rich phase initiates the phase separation process. When the polymer concentration is high, the mentioned

TABLE III
Values Obtained from XRD Analysis

Sample	2θ	*d*	FWHM
α-CD	9.88	10.395	7.4
Polysulfone	7.1	14.456	2.7
α-CD-DMF membrane	8.3	10.653	3.1
α-CD-DMAc membrane	9.88	8.952	3.3
α-CD-DMSO membrane	7.4	11.946	2.3
α-CD-NMP membrane	10.12	8.74	3.8

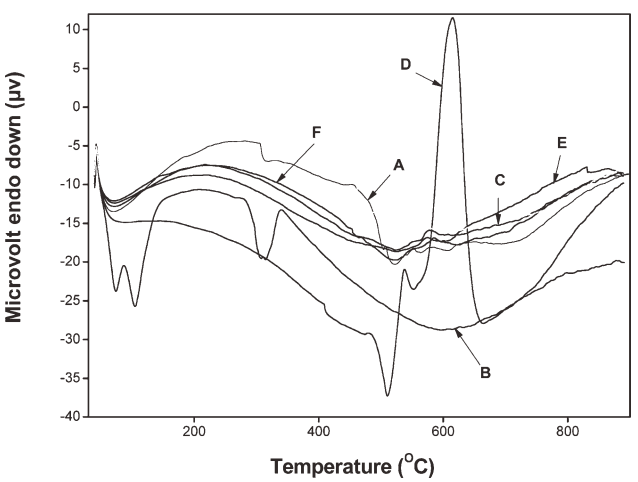

Figure 5 Differential thermogravimetric curves of pure polymer and composite membrane in different casting solvent, A = polysulfone, B = α-cyclodextrin, C = CD-NMP, D = CD-DMF, E = CD-DMAc, F = CD-DMSO.

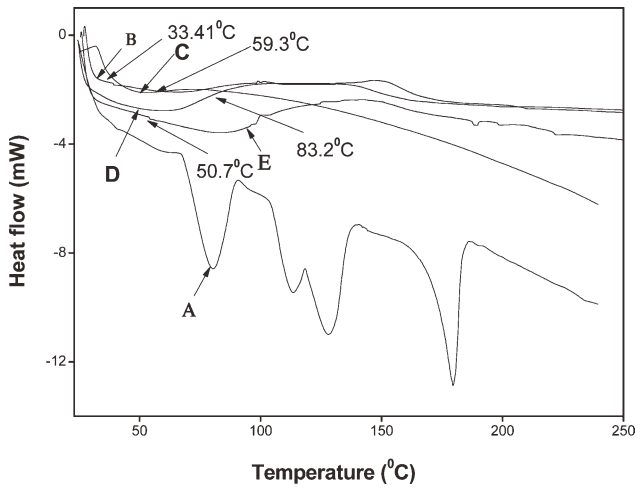

Figure 6 DSC thermograms of pure polymer and composite membrane in different casting solvent, A = α-cyclodextrin, B = CD-NMP, C = CD-DMF, D = CD-DMAc, E = CD-DMSO.

path passes through the bimodal curve above the critical point. In such cases, nucleation of the polymer-lean phase may occur. On the other hand at high polymer concentrations, the precipitation path bypasses the bimodal curve and phenomena such as vitrification, gelation, or crystallization may occur without polymer-lean phase growth. The time of phase separation initiation after immersion is very important to predict the morphology and separation properties of the membrane. If precipitation is initiated immediately after immersion, i.e., instantaneous demixing, the resulting membranes have a porous top layer and if precipitation begins after measurable time, i.e., delayed demixing, the membrane will be a dense skin layer.[26–29] In case of CD-NMP and CD-DMF membranes, precipitation is initiated immediately after immersion and the membranes have porous top layer confirmed by SEM results. In case of CD-DMSO and CD-DMAc membranes, precipitation begins after measurable time (delayed demixing) and the membranes have dense skin layer as is evident from the SEM results.

The formation of the top surfaces is possibly due to demixing of the casting solution by means of nucleation and growth of the polymer-rich phase. Compared to the images of α-CD-DMF, α-CD-DMAc, and α-CD-DMSO membranes, the SEM image of α-CD-NMP membrane shows a more regular image of surface morphology. A more continuous morphology is observed in the surface of this membrane than other membranes. The variation of membrane morphologies observed in the four solvents may be due to the differences in the solvent volatility and the interaction between solvents and α-CD. For rapid evaporation of volatile solvent DMF, it is reported that some grains are produced when the polymer is dissolved in more volatile solvents and can contain large free volume entrapped inside the grains, which cause the formation of large grains.[22] Among the four solvents used in our study DMF is more volatile than other solvents. So α-CD-DMF gives most irregular morphological structure than other membranes studied in this work. However, in case of DMSO, α-CD is dissolved in DMSO at higher temperature; as a result the morphology of α-CD-DMSO membranes is not regular.

In Figure 8(b), the cross-sectional SEM images of NF membranes in different casting solvents are shown. The CD layer is deposited onto the PS layer. It was noticeable that the cross-sectional SEM images, which exhibited a clear variation of CD layer thickness with the variation of casting solvent. Due to the high mutual affinity of the casting solvent for water, instantaneous demixing results, leading to the formation of dense top layer.[23,25] The skin layer of asymmetric membrane is generated from a region with locally elevated polymer concentration.[25] Volatile solvent in the casting dope can rapidly be driven off under-forced convection conditions and thus due to a selective loss of volatile solvent from the outermost surface of the membrane, the polymer-rich regions are forced to coalesce by capillary pressures. This phenomenon causes the polymer-rich phase to undergo rapid vitrification and hence an oriented membrane skin with few pores or defects will be formed.[30,31]

The morphological change of four membranes is also correlated to the polymer–solvent interaction which can be explained by three types of interaction: polymer–polymer, solvent–solvent, and polymer–solvent interactions.

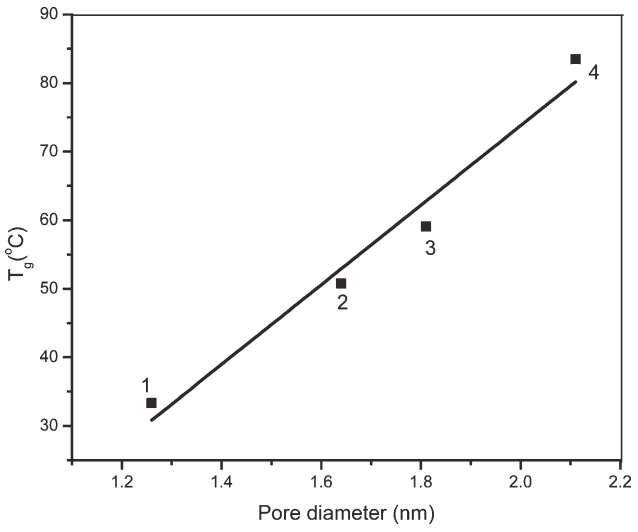

Figure 7 Relationship between glass transition temperature and pore diameter of the membrane, 1: α-CD-NMP, 2: α-CD-DMSO, 3: α-CD-DMF, 4: α-CD-DMAc.

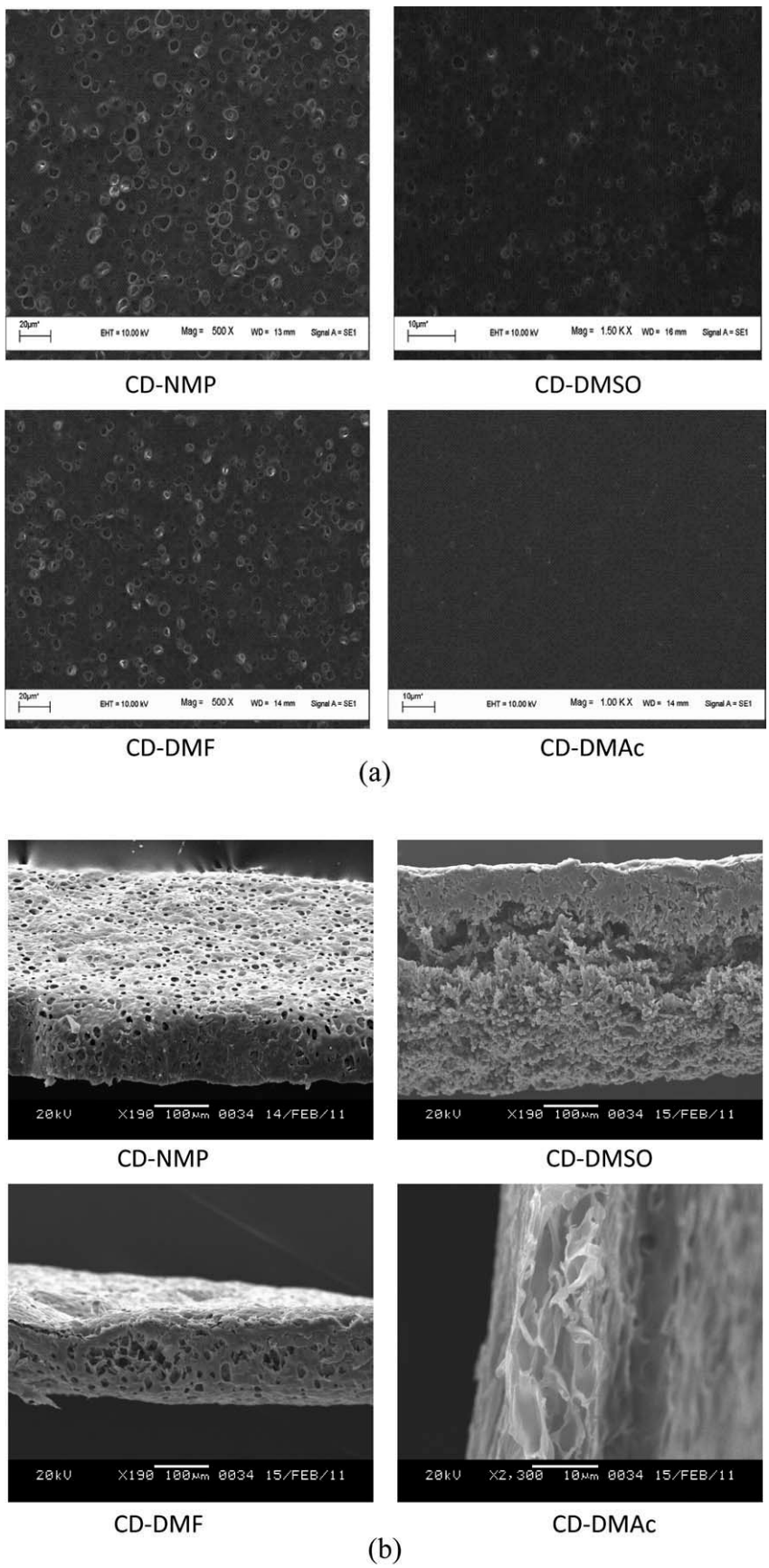

Figure 8 (a): SEM photograph of top surface of NF membrane, (b): cross-sectional SEM photograph of NF membrane.

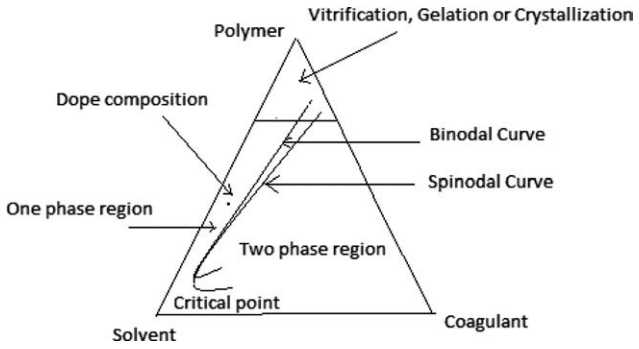

Figure 9 Schematic phase diagram.

Polymer–solvent interaction has been studied for four solvents used in this study. The relative strength of polymer–solvent interactions determines the properties of casting solvent and presumably the morphologies and properties of the final membranes.[32] In a good solvent, the polymer is unfolded, obtaining to the maximum extent, the more favorable polymer–solvent interactions as reported by Guan et al.[21]

Affinity of solvents to polymers can be estimated by introducing the "solubility parameter" δ, which is defined as the square root of the cohesive energy density and described the strength of attractive force between molecules. Polymer–solvent interaction in polymer solutions has been evaluated on the basis of the difference between solubility parameters of polymer and solvents, Hansen took the dispersive forces (δ_d), permanent dipole–dipole interaction (δ_p), and hydrogen bonding forces (δ_H) into consideration.[21] Thus δ is expressed as

$$\Delta^2 = \delta_d^2 + \delta_p^2 + \delta_H^2 \tag{5}$$

The difference in Hansen solubility parameters between solvent and polymer can be calculated by

$$\Delta = [(\delta_{p1,d} - \delta_{s,d})^2 + (\delta_{p1,p} - \delta_{s,p})^2 + (\delta_{p1,H} - \delta_{S,H})]^{1/2} \tag{6}$$

Where P1 and S represent polymer and solvent, respectively. d, p and H represent dispersive, polar, and hydrogen bonding components of Hansen solubility parameters, respectively. d, p, and h represents dispersive, polar, and hydrogen bonding components of Hansen solubility parameters, respectively. In our study, Hansen solubility parameters of four solvents are summarized in Table IV. It is well known that the smaller the difference between the solubility parameters of polymer and solvent, the stronger the polymer–solvent interaction, as reported in literature.[21] Weak polymer solvent interactions cause the more irregular surface morphology of α-CD-DMSO, α-CD-DMF, and α-CD-DMAc membranes compared to α-CD-NMP membrane, which supports the hypothesis that weak polymer–solvent interaction accelerates the further aggregation of grain in some field.[21]

TABLE IV
Hansen Solubility Parameters for Selected Solvents and the Difference in Solubility Parameters between Solvent and α-CD

Solvent	δ_d (MPa)$^{1/2}$	δ_P (MPa)$^{1/2}$	δ_h (MPa)$^{1/2}$	δ (MPa)$^{1/2}$	Δ
NMP	19.4	14.2	13.4	25.05	8.25
DMF	17.4	13.7	11.3	24.9	5.89
DMAc	17.8	14.1	11.8	22.70	7.75
DMSO	18.4	16.4	12.2	24.5	3.44
α-CD	15.2	9.4	7.5	21.12	-

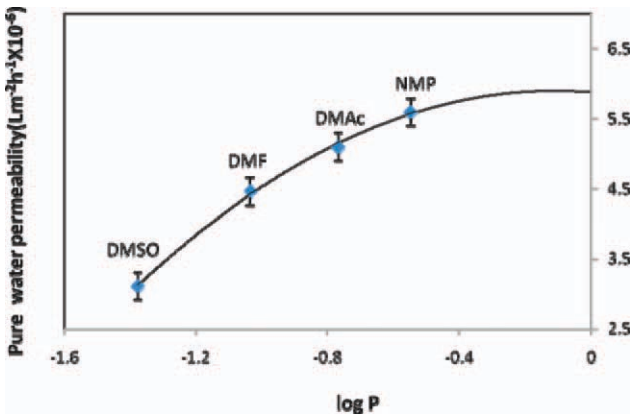

Figure 10 Hydrophobicity of casting solvent as a function of water permeability of the composite membrane. [Color figure can be viewed in the online issue, which is available at wileyonlinelibrary.com.]

Effect of solvent hydrophobicity on water permeability of α-CD membranes

Membrane performance depends on the hydrophobicity of the casting solvent. Solvent hydrophobicity value is the quantitative measure of solvent polarity which is the value of octanol–water partition co-efficient. The correlation of solvent polarity and water permeability of α-CD membrane in different casting solvents is shown in Figure 10. From the figure, it is seen that rate of performance of the composite membranes depends on log *P* value with a significance correlation of straight line.

Effect of casting solvent on the hydrophilicity of membranes

The hydrophilicity of the membrane can be evaluated from the values of water uptake and contact angle measurement, the values of which are given in Table I. The contact angle of a surface against water reflects its wettability which in turn related with the water uptake of membrane. When water wets the surface, i.e., a small contact angle and high water uptake

value, the surface has the ability to interact with water molecules (dipoles) and make the surface more hydrophilic. The contact angle has often been criticized as a surface characterization method of membranes since membrane surfaces usually have pores and they are rough. The surfaces of NF membranes have proven to be very smooth and practically without pores. Therefore, the contact angle measurements would reflect well the hydrophilicity of an NF membrane surface.[33,34] In our case, DMSO is the most polar solvent; however, due to some other interactions of polymer composite and solvent; α-CD-NMP is found to be more hydrophilic in nature.

CONCLUSION

NF membranes have been prepared using four different casting solvents, and the effect of casting solvents on morphologies and performance of the membranes have been studied by means of a series of characterization methods. IR studies of the pure polymer and NF membranes reveal that there are different transition peaks in the pure polymer and composite membranes. XRD study reveals that there are stronger hydrogen bonding interaction which occurred between α-CD-NMP membrane compared to that of other membranes. Thermal decomposition of the pure polymer and composite membranes indicates different range of thermal degradation of each membrane which also indicates a four-step decomposition of the α-CD-NMP membrane. SEM results of the membranes show that membrane morphology can be controlled by changing the casting solvent. The morphological change depends on the demixing behavior of the polymer and solvent volatility combined with polymer–solvent interactions which were measured by considering Hansen solubility parameter. Solvent hydrophobicity is another parameter which effects on the membrane performance in terms of water permeability. Membrane hydrophilicity depends on the value of water uptake and contact angle which is explained in the present study.

Financial support from DST-New Delhi, India, has been gratefully acknowledged. Authors gratefully acknowledge Dr. P. G. Rao, Director, NEIST, Jorhat, for his encouragement to carry out the work.

NOMENCLATURE

W_{wet}	weight of membrane after hydration (mg)
W_{dry}	weight of membrane before hydration (mg)
h	height reached by the liquid (mm)
t	time (s)
R_D	mean hydrodynamic radius of pore (nm)
v	rate of liquid penetration (mm s^{-1})
η	viscosity of the liquid (PaS)
ΔP	pressure difference (Pa)
P	applied pressure (Pa)
γ	surface tension (dynes cm^{-1})
ρ	density (g cm^{-3})
θ	contact angle (°)
R_s	mean static radius (mm)
θ_{eq}	equilibrium contact angle (°)
r_m	mean pore radius (nm)
r_i	radius of pores of different size (nm)
n	number of pores
ε	surface porosity
d_i	pore diameter (nm)
A	area of the membrane (cm^2)
l	thickness of the membrane (mm)
J	permeate flow rate (mmol L^{-1} s^{-1})
T_g	glass transition temperature (°C)
d	dispersive component
p	polar component
h	hydrogen bonding component
F_{STP}	flow rate at standard P_s and temperature T_s
γ_o	volume of sample chamber on the outlet side
T_s	test temperature in Kelvin
p_s	pressure on the outlet side of sample
T	time

REFERENCES

1. Yoo, S. H.; Jho, J. Y.; Won, J.; Park, H. C.; Kang, Y. S. J Indust Eng Chem 2000, 6, 129.
2. Strathmann, H.; Koch, K.; Amar, P.; Baker, R. W. Desalination 1975, 16, 179.
3. Brown, P. J.; Ying, S.; Yang, J. AUTEX Res J 2002, 2, 100.
4. Madaeni, S. S.; Rahimpour, A.; Barzin, J. Iranian Polym J 2005 14, 421.
5. Kim, I. C.; Lee, K.-H. J Appl Polym Sci 2003, 89, 2562.
6. Bodzek, M.; Koter, S.; Owska, K. W. Desalination 2002, 145, 321.
7. Norman, N. L.; Fane, A. G.; Wiston Ho, W. S.; Matsuura, T. In Advanced Membrane Technology and Applications; Li, N. N., Fane, A. G., Winston Ho, W. S., Matsura, T, Eds.; Wiley, INC Publication: New York.
8. Chiang, Y. C.; Hsub, Y. Z.; Ruaan, R. C.; Chuang, C. J.; Tung, K. L. J Membr Sci 2009, 326, 19.
9. Kim, I. C.; Lee, K. H.; Tak, T. M. J Membr Sci 2001, 183, 235.
10. Szejtli, J. Pure Appl Chem 2004, 76, 1825.
11. Farcas, A.; Jarroux, N.; Farcas, A.-M.; Harabagiu, V.; Guegan, P. Digest J Nanomater Biostruct 2006, 1, 55.
12. Uekama, K. J Incl Phenom Macrocycl Chem 2002, 44, 3.
13. Szente, L.; Szejtli, J. Trends Food Sci Technol 2004, 15, 137.
14. Boussu, K.; Van der Bruggen, B.; Vandecasteele, C. Desalination 2006, 200, 416.
15. Rolling, P.; Lamers, M.; Staudt, C. J Appl Membr Sci & Technol 2010, 362, 154.
16. Jiang, L. Y.; Chung, T. S. J Membr Sci 2010, 346, 45.
17. Yilmaz, L.; Mchugh, A. J. J Appl Polym Sci 1986, 31, 997.
18. Altena, F. W.; Smolders, C. A. Macromolecules 1982, 15, 1491
19. www.PMIAPP.COM.
20. Hazarika, S.; Dutta, N. N.; Rao, P. G. J Membr Sci 2006, 2, 13.
21. Guan, H.; Li Dai, C.; Liu, J.; Xu, J. J Membr Sci 2006, 227, 148.
22. Capannelli G.; Vigo F.; Munari S. J Membr Sci 1983, 15, 289
23. Jung, B.; Kim, B.; Yang, J. M. J Membr Sci 2004, 245, 61.

24. Liu, T.; Ozisik, R.; Siegel, R. W. J Polym Sci: Part B: Polym Phys, 2006, 44, 3546.
25. Aroon, M. A.; Ismail, A. F.; Montazer-rahmati, M. M.; Matsuura, T. Sep Purif Technol, 2010, 72, 194
26. Mulder, M. Basic Principles of Membrane Technologies, 2nd ed.; Kluwer Academic Publishers: The Netherlands, 1996.
27. Wang, D. L.; Li, K.; Teo, W. K. J Membr Sci 1995, 98, 233.
28. Mc Kelvey, S. A.; Clausi, D. T.; Koros, W. J. J Membr Sci 1997, 124, 223.
29. Reuvers, A. J.; van den Berg, J. W. A.; Smolders, C. A. J Membr Sci 1987, 34, 45
30. Ismail, A. F.; Dunkin, I. R.; Gallivan, S. L.; Shilton, S. J. Polymer 1999, 40, 6499
31. Iqbal, M.; Man, Z.; Mukhtar, H.; Dutta, B. K. J Membr Sci 2008, 318, 167.
32. Baruah, K.; Hazarika, S.; Chakraverty, A.; Dutta, N. N. Separation of acetic acid from dilute solution by polysulfone cyclodextrin composite nanofiltration membrane (In communication).
33. Kim, B.; Jung, B. Macromol Rapid Commun 2004, 25, 1263.
34. Boussu, K.; Van der Bruggen, B.; Volodin, A.; Van Haesendenck, C.; Delcour, J. A.; Van der Meeren, P.; Vandecasteele, C. Desalination 2006, 191, 245.